

**This item is the archived peer-reviewed author-version of:**

Detection and measurement of picoseconds-pulsed laser energy using a NbTiN superconducting filament

**Reference:**

Harrabi K., Gasmi K., Mekki A., Bahlouli H., Kunwar S., Milošević Milorad.- Detection and measurement of picoseconds-pulsed laser energy using a NbTiN superconducting filament  
IEEE transactions on applied superconductivity / IEEE [New York, N.Y.] - ISSN 1558-2515 - 33:5(2023), 2400205  
Full text (Publisher's DOI): <https://doi.org/10.1109/TASC.2023.3243193>  
To cite this reference: <https://hdl.handle.net/10067/1951100151162165141>

# Detection and measurement of picoseconds-pulsed laser energy using a NbTiN superconducting filament

K. Harrabi,<sup>1,2</sup> K. Gasmi,<sup>1</sup> A. Mekki,<sup>1</sup> H. Bahlouli,<sup>1</sup> S. Kunwar,<sup>1</sup> and M. V. Milošević<sup>3</sup>

<sup>1</sup>*Physics Department, King Fahd University of Petroleum and Minerals, 31261 Dhahran, Saudi Arabia*

<sup>2</sup>*Interdisciplinary Research Center (RC) for Intelligent Secure Systems, KFUPM, Dhahran 31261, Saudi Arabia*

<sup>3</sup>*Department of Physics & NANOLab Center of Excellence, University of Antwerp, Belgium*

(Dated: February 16, 2023)

We investigate non-equilibrium states created by a laser beam incident on a superconducting NbTiN filament subject to an electrical pulse at 4 K. In absence of the laser excitation, when the amplitude of the current pulse applied to the filament exceeds the critical current value, we monitored the delay time  $t_d$  that marks the collapse of the superconducting phase which is then followed by a voltage rise. We linked the delay time to the applied current using the time-dependent Ginzburg-Landau (TDGL) theory, which enabled us to deduce the cooling (or *heat-removal*) time from the fit to the experimental data. Subsequently, we exposed the filament biased with a current pulse close to its critical value to a focused laser beam, inducing a normal state in the impact region of the laser beam. We showed that the energy of the incident beam and the incurred delay time are related to each other by a simple expression, that enables direct measurement of incident beam energy by temporal monitoring of the transport response. This method can be extended for usage in single-photon detection regime, and be used for accurate calibration of an arbitrary light source.

PACS numbers:

## I. INTRODUCTION

Formation of resistive states in superconducting thin filaments has been intensively studied over the last decade due to its importance in ultra-sensitive detection devices [1–3]. Such resistive states stem from the local suppression of superconductivity when the current flowing in the filament exceeds the pair-breaking current of the Cooper pairs, hence creating a non-equilibrium distribution of quasiparticles and causing excess dissipation [4]. The resulting hot-spots are characterized by temperatures greater than the critical temperature of the superconducting filament, before the current is eventually shunted, and heat produced in the dissipative zone is evacuated from the filament to its surrounding environment after a certain delay time [5–7] so that superconductivity is restored. This mechanism is the operational basis of most superconducting single-photon detectors (SNSPD), which are now replacing the conventional single-photon detectors based on photo-multiplier tubes and avalanche photodiodes [8]. SNSPD is considered as detector of choice in communication and in optical signal processing due to its high performance at standard telecom window around 1550 nm and excellent coupling with optical waveguides [9]. Recently, SNSPDs are successfully competing even with indium gallium arsenide single-photon detectors. In particular, SNSPDs have demonstrated an excellent coupling to single-mode optical fibers, very good detection efficiency at the fiber input, low dark-count rate, small timing jitter of few picoseconds, and high counting rate of several megahertz [10]. In addition, the improvements in temporal resolution of single-photon detectors for quantum optical communication systems and in biomedical imaging applications were recently reported in Refs. [11, 12].

As quantum circuits suffer from the limited cooling accessible at the quantum processor stage (below 1 K), fixing the readout device at 4 K stage of the cryostat was proposed as an ultimate solution [13]. It should be noted that hot-spot relaxation time is one of the main parameters that define the maximum count rate of SNSPDs. The working principle consists mainly in generating optically excited hot-spots in superconducting nanowire filaments. When such a superconducting filament absorbs photons, while being biased with a current slightly below its critical threshold value, the photon absorption results in local destruction of superconductivity, i.e., in the formation of the resistive state [8, 14]. In nanostructured superconductors driven by electric current, simulations within the time-dependent Ginzburg-Landau (TDGL) theory have shown that the resistive state is typically characterized by creation and crossing of superconducting vortices, accompanied by local heating [15–17]. In case of resistive state created by the impact of a photon, the threshold current at which the resistive state appears will depend on the energy of the photon [18], but also on geometric considerations. Namely, in the case of meandering superconducting filaments crossing vortices are instigated when the photons are absorbed near the corners where the current is maximal due to geometric crowding [19]. Whereas the photon action away from the corners where the current distribution is more uniform induces the resistive state by hot-spot formation [20]. Dissipative phase-slip states were created by an electrical current pulse in a NbTiN filament [21], where the temperature attained at the center of the hot spots or phase-slip centers based on the radiation model were determined [22]. Moreover the analysis aimed at determination of the minimum hotspot current was investigate for NbTiN filament [23].

In the present work we study the onset of resistive

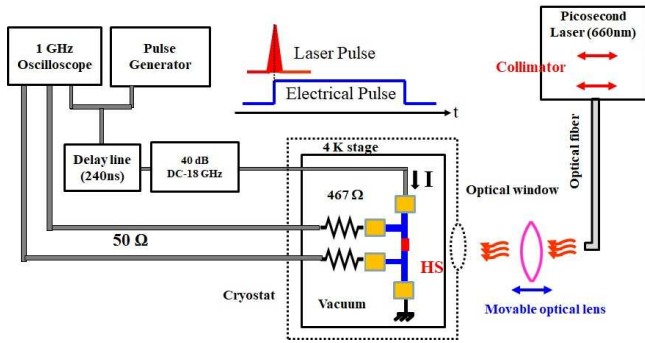


FIG. 1: Schematics of the experimental setup. A pulse generator biases the filament with an electrical pulse with a rise time is 1.2 ns (AVTECH company). An oscilloscope is used to monitor the voltage and to determine the delay time  $t_d$ . The laser beam was directed through an optical window to the center of the sample, and was synced to fall at the rise time of the electrical pulse.

state in a NbTiN superconducting filament driven by an electrical current pulse, with a first goal to deduce the heat-escape time. In the next stage, the NbTiN superconducting filament operating at 4 K was biased with an electrical current pulse slightly below its critical current, and exposed to a localized excitation by a picoseconds-pulsed laser beam. A modulated weak amount of energy delivered by a short laser pulse is still sufficient to yield suppression of superconductivity and a voltage signal across the sample after a certain delay time  $t_d$  corresponding to the absorption of the incident energy. The filament is systematically illuminated by different laser energies resulting in different delay times at the onset of the resistive state. The main goal of the present work is to connect the incident laser energy and the resulting delay time  $t_d$  into a convenient functional dependence, so that transport measurements on superconductors can be used to detect the absorbed energy of incident radiation, and/or calibrate light sources to which a superconducting sensor is exposed.

## II. EXPERIMENTAL SETUP

The NbTiN filament was sputtered on a sapphire substrate (STAR-Cryoelectronics, NM, USA). The gold contact pads on the sample were patterned using standard photo-lithographic and ion-milling processes. In the present experiment, 20 nm thick,  $w = 5 \mu\text{m}$  wide NbTiN strips were investigated below their superconducting transition temperatures, under vacuum. The made design has the main strip and two lateral probes that are 600  $\mu\text{m}$  apart from each other.

The filament was cooled below its critical temperature  $T_c = 7.8 \text{ K}$  and excited by an electrical current pulse with a duration of 450 ns and with a repetition frequency of 10 kHz. A high-frequency attenuator and 50  $\Omega$  coaxial cables were used in the experimental setup. A reflected

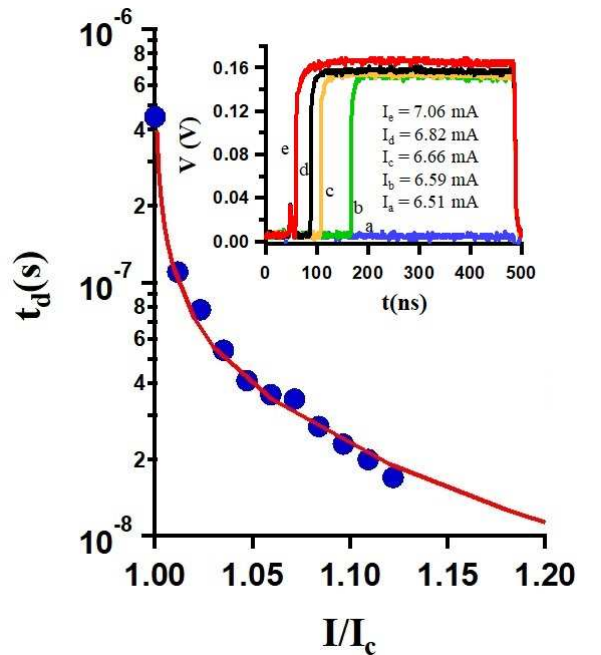


FIG. 2: Experimental delay times (blue dots, log scale) versus the applied current (scaled to the critical current) at  $T = 4 \text{ K}$ . The theoretical curve [following Eq. (1)] is adjusted to fit the experimental data with a pre-factor  $\tau_d = 4.3 \text{ ns}$ . The inset figure shows the temporal voltage response to different applied current values. The small peak that appears in the voltage response is related to the wire inductance that connects the coaxial cable to the sample on the substrate.

negative pulse is created as a consequence of an incident pulse in the superconducting state. The two pulses are separated from each other using air-delay line. Two lateral probes were used to measure the voltage across the filament. To reduce the current leakage to the oscilloscope for currents higher than  $I_c$  where voltage develops, two 467  $\Omega$  resistors were added in series with the lateral probes.

## III. NON-EQUILIBRIUM STATES INDUCED BY ELECTRICAL CURRENT PULSE

The resistive states can be created in superconducting filaments using an electrical pulse with current values exceeding the critical current  $I_c$ . Under short-pulsed current, a localized zone of the sample may turn into a normal state, in contrast to a continuous overcritical current where the entire filament is eventually brought to the normal state owing to the steady heating effects. It was reported earlier that different dissipative modes may occur depending on the sample specification [24]. The main dissipative mechanisms are identified as hot-spots and phase-slip lines (PSLs) that are most likely to appear in absence of applied magnetic field (where also vortex flow regime becomes relevant). The PSL is usu-

ally considered as a localized region of intermittent (and fast changing) suppression and recovery of the superconducting condensate, mimicking an extremely fast vortex crossing the sample. Originally PSLs were considered in one-dimensional superconducting wires with widths ( $w$ ) comparable to the coherence length  $\simeq \xi$  [4], where phase-slip ‘center’ (PSC) is a more appropriate name. The same type of dissipation develops in wider filaments as well ( $w \gg \xi$ ), acquiring an analogous behaviour as described above, that becomes a moving PSC, i.e. a phase-slip line (PSL) [7, 25].

As first reported in Ref. 26, an electrical current pulse excitation results in the appearance of a voltage for currents that exceed the critical current in aluminium filament with a controllable delay time  $t_d$  [26]. Hot-spots and PSLs in that case could be singled out due to their distinct behavior under an overcritical current pulse. Both mechanisms caused a voltage appearance after a variable delay time  $t_d$  and for current amplitude higher than  $I_c$ . The hot-spot is then recognized as a growing dissipative structure and is characterized by a monotonic voltage versus time growth. Contrarily, a formed PSL is a stable resistive state that is characterized by a constant voltage over time (for efficiently removed excess heating).

The breakdown of the superconductivity according to above scenarios can be performed in experiment in several different manners. The one adopted in our experiment for the purpose of this section is to send an electrical current pulse larger than  $I_c$ . We identified the critical current as the smallest value giving rise of 1 microvolt in the voltage response. In that case, a voltage develops after a delay time  $t_d$  that is controlled by the amplitude of the applied current. The analytic expression of the delay time in such a scenario can be derived from the TDGL theory, and is expressed by [4]:

$$t_d(I/I_c) = \tau_d \int_0^1 \frac{2f^4 df}{\frac{4}{27}(\frac{I}{I_c})^4 - f^2 + f^6}. \quad (1)$$

Here  $f$  represents the time-averaged Cooper-pair density at the PSL, and  $I_c$  and  $I$  are the critical and applied currents, respectively. The parameter  $\tau_d$  is related to the electron-phonon scattering time. It was confirmed in earlier works that it depends strongly on the film thickness, and it was identified to be the filament cooling (or heat-removal) time [27, 28].

In our experiment, the superconducting filament was studied at 4 K, and the delay time  $t_d$  was measured for different applied current values larger than the critical current. The obtained data was fitted using Eq. (1), and the parameter preceding the integral was extracted from the best fit as shown in Fig. 2. For the present NbTiN film with a thickness  $\delta = 20$  nm we deduced  $\tau_d = 4.3$  ns as the time required to revive the superconducting state in the localized PSL zone. This parameter is related to the thermal relaxation time that is related to the phonon cooling time. It mainly depends on the interface between the superconducting filament and the substrate. We conducted measurements in the past on Nb filaments that

showed 2 ns for a 20 nm thick filament [28]. In addition, in a pulse photo-resistance experiment, a similar ratio  $\tau_{esc}/b = 8$  ps/nm for a 20 nm thick NbN film was reported in Ref.[29].

#### IV. OPTICAL ENERGY DETECTION

Next the same NbTiN filament was maintained below its superconducting critical temperature  $T_c$ , but was biased with a current  $I_b$  slightly below the superconducting critical value ( $\lesssim I_c$ ), and exposed to a laser beam that will drive the filament into a resistive state. The laser beam is brought directly onto the sample (filament) using an optical fiber. After removal of the optical (glass) window at the top of the vacuum chamber, the laser power is then measured exactly at the level of the sample using a power meter. Here, the power head of the power meter is placed exactly at the height of the sample. Namely, a weak laser beam intensity was focused on the sample through a quartz window using an optic collimator, a single-mode optical fiber and a focusing lens. The laser source used was a picosecond-pulsed diode laser from PICOQUANT (Mod LDH-P-C-650, PDL 800-B), emitting in the red spectral range ( $\lambda = 660$  nm), with a full width

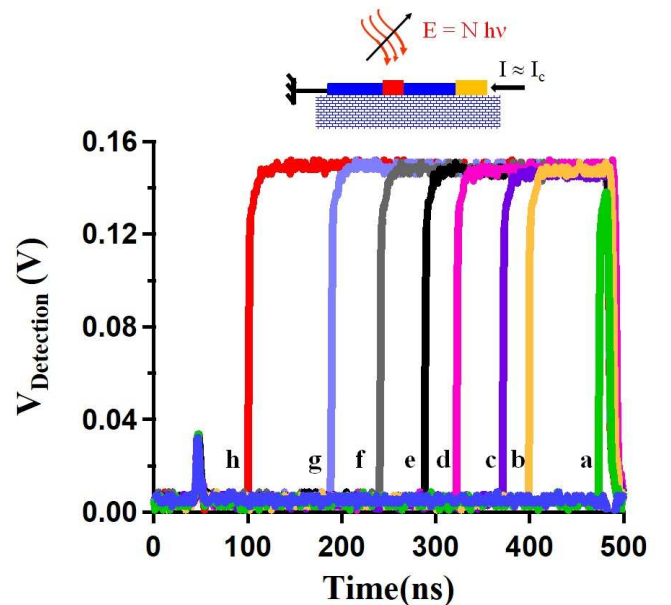


FIG. 3: Voltage detected along the superconducting filament biased with a current just below the critical pulse value ( $I_b \simeq I_c = 6.51$  mA) in presence of a laser pulse excitation (for  $\Delta t = 50$  ps,  $\lambda = 660$  nm). The delay times correspondingly follow the amount of energy absorbed by the filament is increased in different cases. As the energy intensity of the laser is increased the delay time is reduced (traces a to h). Dark blue curve represents the signal when the laser is off. Top inset shows schematic illustration of detection, where  $N$  is a (large) number of photons.

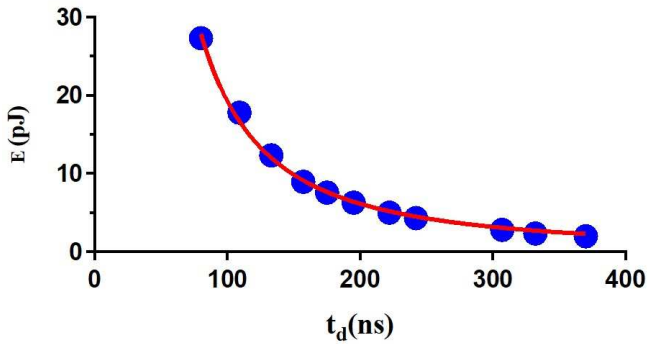


FIG. 4: The amount of energy (blue dots) sent through the superconducting filament biased with current  $I_b \simeq I_c$ , plotted against the corresponding delay times  $t_d$ . The red solid curve shows the fitting function from Eq. (2), where  $E_0 = 0.1$  pJ,  $A = 4.1 \times 10^4$  pJ.(ns) $^{-5/3}$ , and  $\alpha = 5/3$ .

at half maximum (FWHM) of about 50 ps. The output power and pulse duration of the laser were both adjustable via a driver unit. The coupling to the single-mode optical fiber allows transforming the elliptical beam shape into a Gaussian shaped beam at the output of the fiber. In the present experiment, the detection mechanism of the laser incidence is different from the conventional one used for single-photon detection. In the common detection process, one photon breaks Cooper pairs where a hot-spot is generated, and the applied current is deviated left and right aside the hot-spot. There current density increases and induces a normal-state zone that gradually extends across the width of the filament.

However, in our experiment, we used a laser spot readily adjusted to cover the full width of the filament. Therefore the photon flux is absorbed within the entire width, hence destroying Cooper pairs across the filament and expanding to a certain length along the filament due to the electrical biasing pulse. When the laser beam is blocked, the filament remains in the superconducting state as shown by the dark blue curve in Fig. 3. However, when the laser beam is allowed to hit the sample, the illuminated area of the sample becomes a normal hot-spot where superconductivity is locally suppressed and generates a significant output voltage pulse after a certain delay time  $t_d$ .

Curves *b* to *h* in Fig. 3 show the temporal voltage response of the filament to a varied amount of energy generated by the laser pulse calibrated by a power meter device, each exhibiting a corresponding delay time  $t_d$ . The amount of energy absorbed in the filament biased with a current slightly below the critical current creates a resistive state. This process bears similarities to the case of biasing with currents greater than the critical current. The observed delay times  $t_d$  are reduced for increasing energy intensities of the laser beam. We find that the incident beam energy and the incurred delay times are conveniently related to each other by a power-law depen-

dence given by

$$E = E_0 + At_d^{-\alpha}, \quad (2)$$

where  $E_0$ ,  $A$  and  $\alpha$  are the fitting parameters. The beam energies sent to the sample versus the corresponding induced delay times  $t_d$  are plotted in Fig. 4, along with the best fit by Eq. (2) (obtained with  $E_0 = 0.1$  pJ,  $A = 4.1 \times 10^4$  pJ.(ns) $^{-5/3}$ , and  $\alpha = 5/3$ ). The long delay time  $t_d$  corresponds to a weak amount of energy radiation absorbed by the superconducting filament. Conversely, the short delay time  $t_d$  is attributed to strong absorption of radiation energy. In fact, the calibration curve shown in Fig. 4 is similar to the one used for measuring the temperature using a semiconductor or metal-oxide thermometer. The fitting function can be extrapolated to cover the entire range of the pulse length, and therefore it corresponds to strong and weak amounts of energies. The detection of single photons having different wavelengths is also manageable by adopting this technique. The present device would therefore allow one not only to detect the absorbed optical energy, but it could also be used to measure and calibrate any laser source with high accuracy. In the present effort, we were limited to relatively short delay times corresponding to a large amount of energy detection. However, longer delay times would be possible to access using optical filters, enabling detection of much lower energies than in this first report.

## V. CONCLUSION

In summary, we have investigated the out-of-equilibrium resistive state generated by a localized picosecond pulsed laser beam in a 20 nm-thin and 5  $\mu$ m wide NbTiN superconducting filament carrying an applied current. Temporal voltage data in experiments using overcritical current pulses allowed us to model the delay time using a theoretical expression derived from TDGL theory, and thereby identifying the characteristic cooling time of the filament to be about 4.3 ns. As a next step, we biased the same filament with a current slightly below the critical current, and measured the onset of the resistive state when exposed to an incident laser beam with 50 ps pulses and varied intensity. For each laser intensity used, the absorbed amount of energy was detected through an output voltage rising after a delay time  $t_d$  and noticed that this delay time gets shorter as the absorbed energy is increased. We demonstrated that the experimentally recorded delay time is connected to the laser intensity energy used through a simple power-law dependence, that can be adopted as a calibration curve for measuring the amount of energy absorbed by the superconductor down to picoJoule level, or to back-track the properties of the unknown incident beam. More generically, the measurement of delay time of the created resistive state in superconducting filaments can be used to calibrate an arbitrary light source, even in cases involving very weak energy absorption. This confirms that the

present methodology constitutes a promising technique to be deployed for single-photon detection.

project DF191008 .

## ACKNOWLEDGMENTS

This work was supported by the King Fahd University of Petroleum and Minerals, Saudi Arabia, under the DSR

- 
- [1] N.G.N. Constantino, M.S. Anwar, O.W. Kennedy, M. Dang, P.A. Warburton, J.C. Fenton, *Nanomaterials* **8**, 442 (2018). Emergence of Quantum Phase-Slip Behaviour in Superconducting NbN Nanowires: DC Electrical Transport and Fabrication Technologies
- [2] Y. Chen, Y-H, Lin, S. D. Snyder, A.M. Goldman, and A. Kamenev, *Nat. Phys.* **10**, 567 – 571 (2014). Dissipative superconducting state of non-equilibrium nanowires
- [3] I. Madan *et al.*, *Sci. Adv.* **4**, 0043 (2018). Nonequilibrium optical control of dynamical states in superconducting nanowire circuits
- [4] M. Tinkham, *Intro. to Superconductivity*, 2nd ed. (McGraw-Hill, Singapore, 1996), Chap. 11.
- [5] S. Ferrari *et al.*, *Opt. Express* **25**, 8739 (2017). Hot-spot relaxation time current dependence in niobium nitride waveguide-integrated superconducting nanowire single-photon detectors
- [6] W.J. Skocpol, M.R. Beasley, M. Tinkham, *J. Low Temp. Phys.* **16**, 145 (1974). Phase-slip centers and nonequilibrium processes in superconducting tin microbridges
- [7] V.G. Volotskaya, I.M. Dmitrenko, and A.G. Sivakov, *Sov. J. Low Temp. Phys.* **10**, 179, (1984). New resistive state of wide superconducting films
- [8] A. Stockhausen, K. Il'in, M. Siegel, U. Sädervall, P. Jedrasik, A. Semenov, and H.-W. Hübers, *Supercond. Sci. Technol.* **25**, 035012 (2012). Adjustment of self-heating in long superconducting thin film NbN microbridges
- [9] X. Hou *et al.*, *Opt. Express* **29**, 7746 (2021). Waveguide-coupled superconducting nanowire single-photon detectors based on femtosecond laser direct writing
- [10] J.P. Allmaras, A.G. Kozorezov, B.A. Korzh, K.K. Berggren, and M.D. Shaw, *Phys. Rev. Appl.* **11**, 034062 (2019). Intrinsic Timing Jitter and Latency in Superconducting Nanowire Single-photon Detectors
- [11] B. Korzh *et al.*, *Nat. Photonics* **14**, 250 (2020). Demonstration of sub-3 ps temporal resolution with a superconducting nanowire single-photon detector.
- [12] I.E. Zadeh, J. Chang, J.W.N. Los, S. Gyger, A.W. Elshaari, S. Steinhauer, S.N. Dorenbos, and V. Zwiller, *Appl. Phys. Lett.* **118**, 190502 (2021). Superconducting nanowire single-photon detectors: A perspective on evolution, state-of-the-art, future developments, and applications
- [13] R. Gougues, J.W.N. Los, J. Zichi, J. Chang, N. Kalhor, G. Bulgarini, S.N. Dorenbos, V. Zwiller, and I.E. Zadeh, *Opt. Express* **27**, 24601 (2019). Superconducting nanowire single photon detectors operating at temperature from 4 to 7 K
- [14] G.N. Gol'tsman, O. Okunev, G. Chulkova, A. Lipatov, A. Semenov, K. Smirnov, B. Voronov, A. Dzardanov, C. Williams, and R. Sobolewski, *App. Phys. Lett.* **79**, 705 (2001). Picosecond superconducting single-photon optical detector
- [15] G.R. Berdiyrov, M.V. Milošević, and F.M. Peeters, *Phys. Rev. B* **79**, 184506 (2009). Kinematic vortex-antivortex lines in strongly driven superconducting stripes
- [16] A.V. Silhanek *et al.*, *Phys. Rev. Lett.* **104**, 017001 (2010). Formation of Stripelike Flux Patterns Obtained by Freezing Kinematic Vortices in a Superconducting Pb Film
- [17] G.R. Berdiyrov *et al.*, *Phys. Rev. Lett.* **109**, 057004 (2012). Magnetoresistance Oscillations in Mesoscopic Superconductors due to Current-Excited Moving Vortices
- [18] D.Yu. Vodolazov, *Phys. Rev. B* **90**, 054515 (2014). Current dependence of the red boundary of superconducting single-photon detectors in the modified hot-spot model
- [19] G.R. Berdiyrov, M.V. Milošević, and F.M. Peeters, *Appl. Phys. Lett.* **100**, 262603 (2012). Spatially dependent sensitivity of superconducting meanders as single-photon detectors
- [20] J.R. Clem, Y. Mawatari, G.R. Berdiyrov, and F.M. Peeters, *Phys. Rev. B* **85**, 144511 (2012). Predicted field-dependent increase of critical currents in asymmetric superconducting nanocircuits
- [21] K. Harrabi, *AIP ADVANCES* **5**, 037102 (2015). Resistive states created in superconducting NbTiN filaments by an electrical current pulse
- [22] K. Harrabi, F. O. Bakare, F. Oktasendra, J. P. Maneval, *J. Supercond. Nov. Magn.* **30**, 1349 (2017). Temperature Dependence of the Phonon Escape Time Deduced from the Nucleation Time of Phase Slip Center in Superconducting NbTiN Thin Film
- [23] K. Harrabi, A. Mekki, S. Kunwar, and J. P. Maneval, *J. Appl. Phys.* **123**, 083901 (2018). Pulse measurement of the hot spot current in a NbTiN superconducting filament
- [24] K. Harrabi, *J. Supercond. Nov. Magn.* **28**, 573 (2015). Temperature Elevation of Current-Driven Phase-Slip Centers in YBa<sub>2</sub>Cu<sub>3</sub>O<sub>7</sub> Strips
- [25] A.G. Sivakov *et al.*, *Phys. Rev. Lett.* **91**, 267001 (2003). Josephson Behavior of Phase-Slip Lines in Wide Superconducting Strips
- [26] J.A. Pals and J. Wolter, *Phys. Lett. A* **70**, 150 (1979). Measurement of the order-parameter relaxation in superconducting Al-strips
- [27] G. Berdiyrov, K. Harrabi, F. Oktasendra, K. Gasmi, A. I. Mansour, J.P. Maneval, and F.M. Peeters, *Phys. Rev.* **90**, 134505 (2014). Parametric amplification of vortex-antivortex pair generation in a Josephson junction
- [28] K. Harrabi, F. Oktasendra, K. Gasmi, G. Berdiyrov, A. Mekki, and J.P. Maneval, *IEEE Trans. Appl. Supercond.* **26**, 7399353 (2016). Phonon Escape Time Deduced From

the Time of Nucleation of Hot Spots in Superconducting Niobium Filaments

[29] A. D. Semenov *et al.* Phys. Rev. B 52, 581 (1995). Analy-

sis of the nonequilibrium photoresponse of superconducting films to pulsed radiation by use of a two-temperature model